Extracting Photon PDF and Proton PDFs at an EIC

Xiaoxuan Chu 褚晓璇

USTC, 9/11/2018

Outline

1. Possible realizations of an EIC
2. Photon structure studied at eRHIC
   - Motivation and Introduction
   - (Un)polarized photon structure
   - Calculation of the underlying events effect
3. Extracting proton PDFs from EIC by a global analysis
4. Summary and outlook

Questions an EIC aims to answer

The core questions described in the EIC white paper

- How are the sea quarks and gluons, and their spins, distributed in space and momentum inside the nucleon? - Polarization
- How do color-charged quarks and gluons distributed with a nuclear medium? - A range of center of mass energies & High Luminosity
- What happens to the gluon density in nuclei? Where does the saturation of gluon densities set in? - Ion beams

These questions call for facilities with capabilities that far exceed any current or past colliding beams accelerator facility: Electron Ion Collider (EIC)

Deep Inelastic Scattering

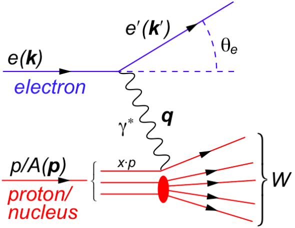

$$Q^2 = sxy$$

- s: center-of-mass energy squared
- Q^2: Resolution power
- x: The fraction of the nucleon's momentum carried by the struck quark
- y: Inelasticity

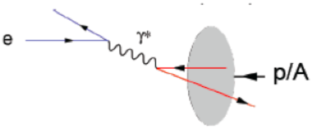

- Electron beams provide point-like probe - resolution
- Direct, model independent determination of partonic kinematics of physics processes
- High precision & access to partonic kinematics through scattered lepton

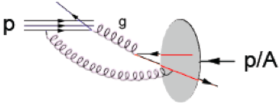

- Probe has complex structure
- No simple access to partonic kinematics

Physics cases of EIC in US

eRHIC @ BNL

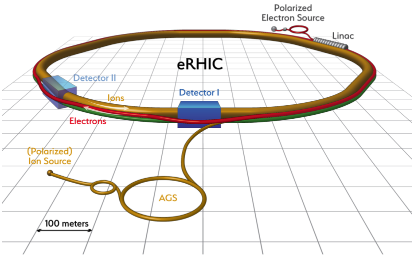

JLEIC @ JLAB

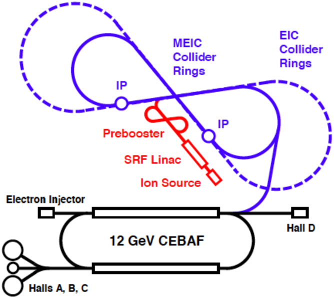

eRHIC:

- Center-of-mass energy (Ecm) of (29-140) GeV
- A luminosity of up to 10^{34}cm^{-2}s^{-1}
- High polarization of electron and ion beams with frequent changes to the spin direction with polarizations well above 70%
- Collisions of electrons with a large range of light to heavy ions (protons to Gold ions)

Photon structure studied at EIC: Motivation

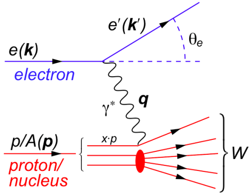

- Behavior of the exchanged photon: direct photon state, resolved photon state
- The “internal structure” of photons is a manifestation of quantum fluctuations: photon splits into parton content
- Photoproduction: low Q^2
- Parton Distribution Functions(PDFs) of Photon: q(x,Q^2), g(x,Q^2)

Resolved state

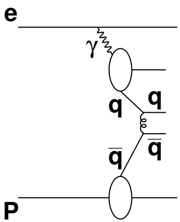

Direct state

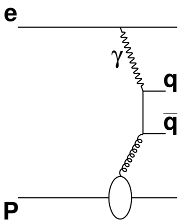

Motivation: Existing experiment results

[arXiv:9504004, arXiv:9710018, Eur. Phys. J. C 10, 363-372 (1999), DESY 97-164]

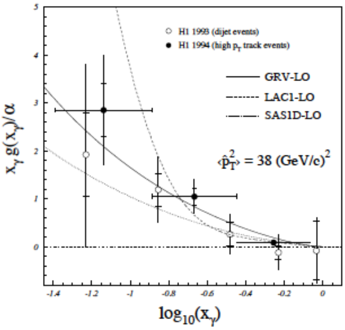

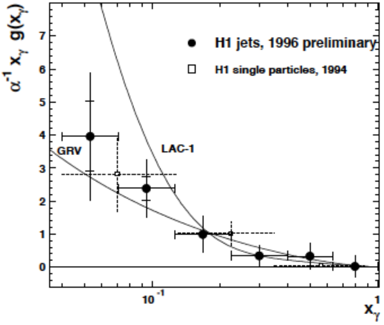

- Lack of statistic, especially in the small x_γ region which is important for the constrain of photon PDFs.
- Results from jet and charged particle measurements show that the best fit are GRV and SAS
- The nature of e^+e^- collisions is two photon physics, the photon structure is very important for ILC $\gamma\gamma$ option.
- Polarized photon PDFs are never measured before.

Low Q^2 tagger

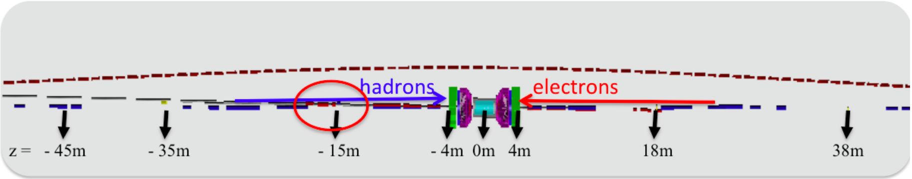

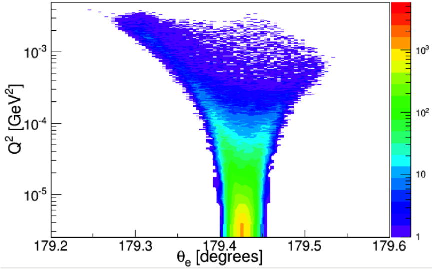

- Outgoing electrons are reconstructed in the tagger
- Acceptance for electrons is down to 10^{-5} GeV^2

Di-jet measurment

Resolved process

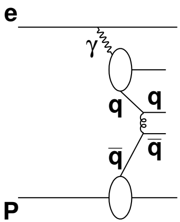

Direct process

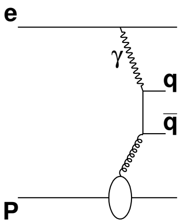

- How to separate: Resolved: $x_\gamma < 1$; direct: $x_\gamma = 1$.
  $x_\gamma^{rec} = \frac{1}{2E_e y}(p_{T1}e^{-\eta_1} + p_{T2}e^{\eta_2})$, $y = \frac{E_\gamma}{E_e}$.
- Parton densities can be extracted by measuring di-jet cross section:
  $\frac{d^2\sigma}{dx_\gamma dQ^2} = \gamma_{flux} \otimes f_\gamma(x_\gamma, Q^2, \mu) \otimes f_p(x_p, \mu) \otimes \sigma_{ij}$,
  γ_{flux} is calculable in QED, f_p is the PDF of the proton, σ_{ij} is the cross section of the hard process, which is calculable in pQCD

Reproduce HERA data

Reproduce the inclusive cross section, photon PDF set is SAS, proton PDF is CTEQ5m, $10^{-5}\text{GeV}^2 < Q^2 < 1\text{GeV}^2$, $L = 1\text{fb}^{-1}$.

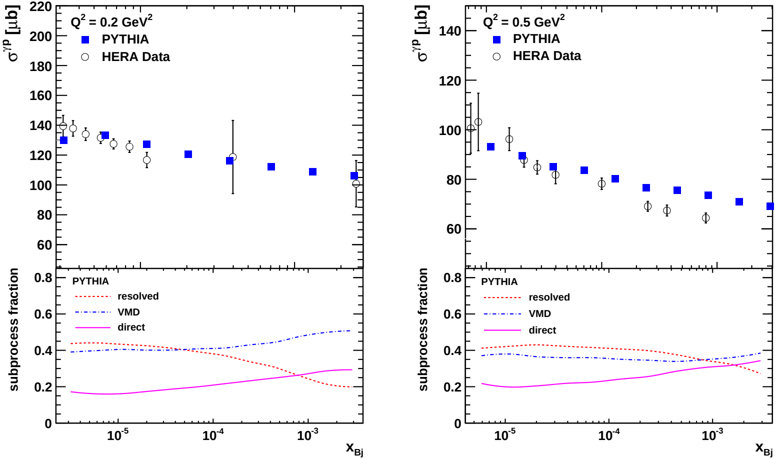

[HERA Data: Phys. Rev. D 96 014001(2017)]

Reproduce HERA data

Reproduce the di-jet cross section, photon PDF set is SAS, proton PDF is CTEQ5m, $10^{-5}\text{GeV}^2 < Q^2 < 1\text{GeV}^2$.

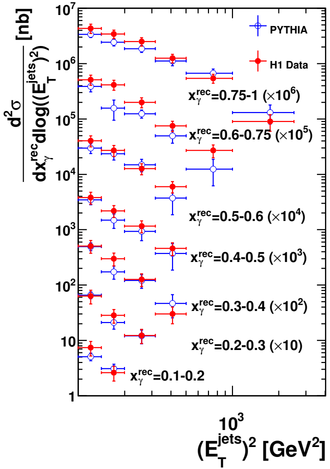

- Kinematics cuts from HERA: 27.5GeV×820 GeV, $0.2 < y < 0.83$, $|\Delta\eta^{jets}| < 1$, $0 < \eta^{jet1} + \eta^{jet2} < 4$, $E_T^{jet1}, E_T^{jet2} > 7.5\text{GeV}$, $E_T^{jet1} + E_T^{jet2} > 20\text{GeV}$, $|E_T^{jet1} - E_T^{jet2}|/(E_T^{jet1} + E_T^{jet2}) < 0.25$
- Our simulation can match the existing data

Unpolarized photon structure at EIC

20GeV×250 GeV, $0.01 < y < 0.95$, two highest p_T jets, $p_T^{\text{jet1}} > 5$GeV, $p_T^{\text{jet1}} > p_T^{\text{jet2}} > 4.5$ GeV, $|\eta^{\text{jets}}| < 4.5$, stable particle $p_T > 250$ MeV.

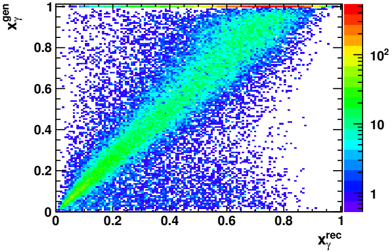

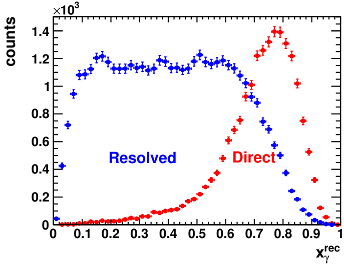

Di-jet method provides a good way to reconstruct x_γ, we can separate resolved/direct process($x_\gamma^{\text{rec}} < 0.6$).

Unpolarized photon structure at EIC

20GeV$\times$250 GeV, $0.01 < y < 0.95$, two highest p_T jets, $p_T^{\text{jet1}} > 5$GeV, $p_T^{\text{jet1}} > p_T^{\text{jet2}} > 4.5$ GeV, $|\eta^{\text{jets}}| < 4.5$, stable particle $p_T > 250$ MeV.

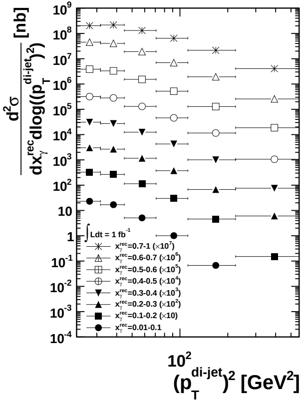

The simulation shows the capability to measure the cross section for di-jet production at $\int L = 1\ \text{fb}^{-1}$, with high accuracy in a wide kinematic range at EIC and extract the unpolarized photon PDFs from a global fit.

EIC advantages compared to HERA

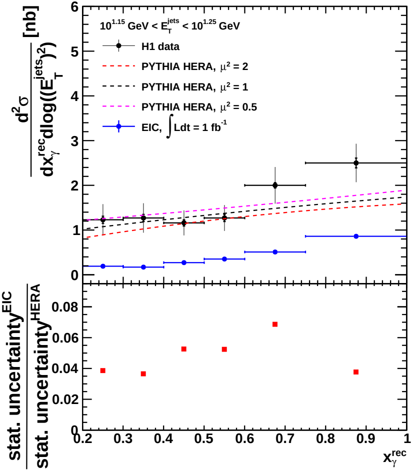

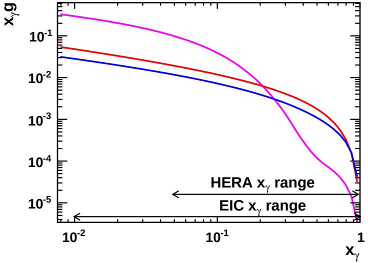

- High luminosity to define the uncertainty band
- Feasiblity to probe small x_γ region

Method of flavor tagging

The photon is in the hadronic state, can we expect to know the information of the parton content inside the photon?

- $\frac{d^2\sigma}{dx_\gamma dQ^2} = \gamma_{flux} \otimes f_\gamma(x_\gamma, Q^2, \mu) \otimes f_p(x_p, \mu) \otimes \sigma_{ij}$
- From measuring the di-jet cross section, we can extract the total PDFs of the photon.
- We search the possibility of q/g discrimination. (will be discussed later)
- We do flavor tagging to achieve the goal of separating the contribution from different flavor partons.

Method of flavor tagging

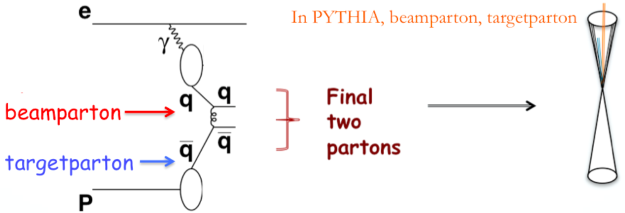

We will separate q/g jet first and select the jet from the parton which has the same flavor as the beamparton, which is marked with "jet from the photon side".

How to choose the jet from the photon side

hadrons, $\eta_{\mathrm{Lab}}>0$ → ← electrons, $\eta_{\mathrm{Lab}}<0$

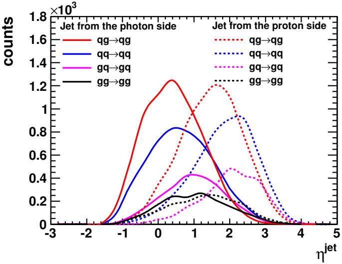

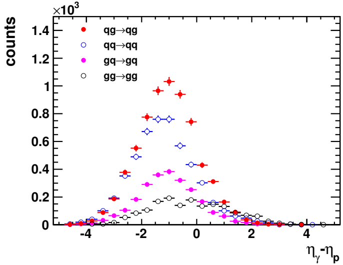

- Conclusion: Influenced by the moving direction of the incoming electrons, the jets from the photon which is radiated from the electron, the pseudo-rapidity of jet from the photon is smaller than that of proton side jet
- What we can do in the experiment: take the jet with smaller η as the photon side jet

Flavor tagging

The correlation between the beamparton flavor and the type of the leading hadron inside photon side jet.

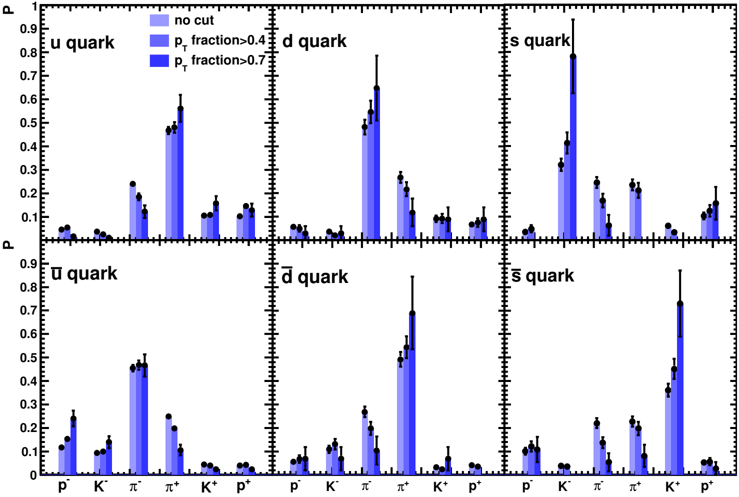

Flavor tagging

The correlation between the beamparton flavor and the type of the leading hadron inside photon side jet.

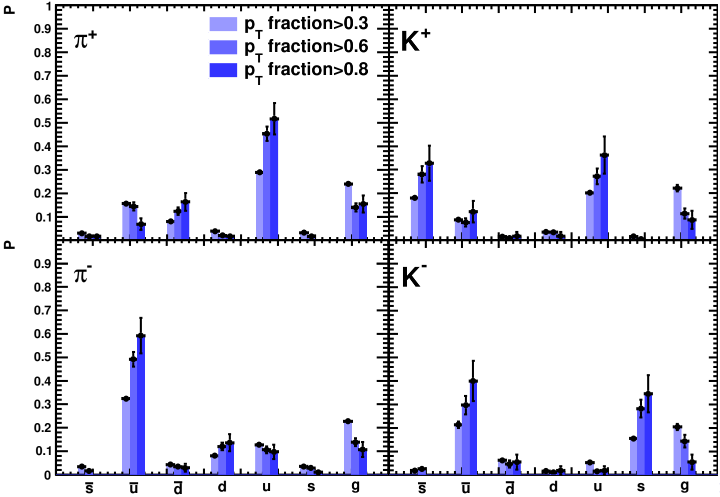

What is the behavior of the photon if we add spin on it?

Polarized photon PDFs

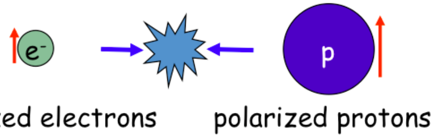

Input for polarized ep collision

pol. photon PDFs	min: $\Delta f^\gamma = 0$; max: $\Delta f^\gamma = f^\gamma$
pol. proton PDF	DSSV

$A^\gamma = \Delta f^\gamma / f^\gamma$

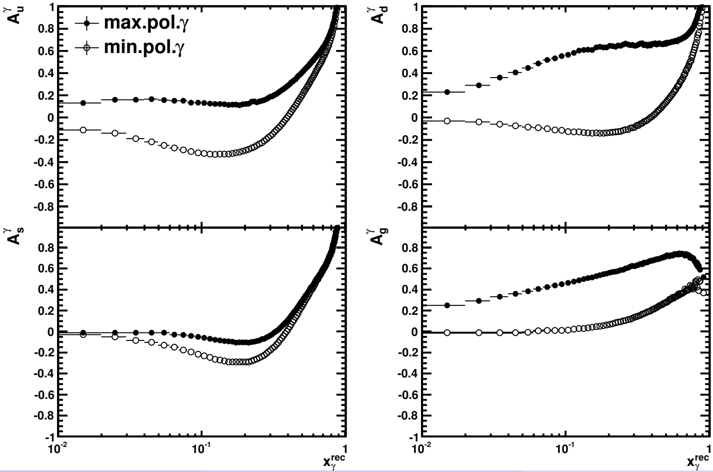

Polarized photon structure

$$\frac{d^2\Delta\sigma}{dx_\gamma dQ^2} = \Delta\gamma_{flux} \otimes \Delta f_\gamma(x_\gamma, Q^2, \mu) \otimes \Delta f_p(x_p, \mu) \otimes \sigma_{ij}$$

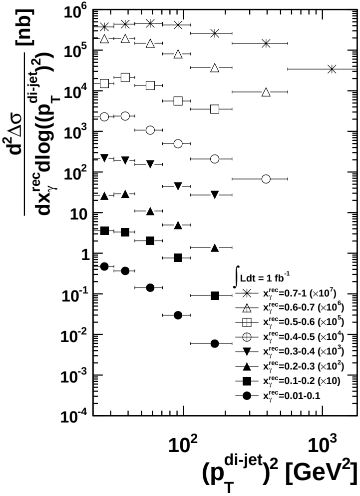

$$\Delta\sigma = \frac{1}{2}(\sigma^{++} - \sigma^{+-})$$

- The simulation shows the capability to measure the polarized cross section for di-jet production, with high accuracy in a wide kinematic range at EIC.
- First measurement of polarized photon PDFs with high precision.
- Flavor tagging can also be applied in polarized case.

$A_{LL} = \Delta\sigma/\sigma$

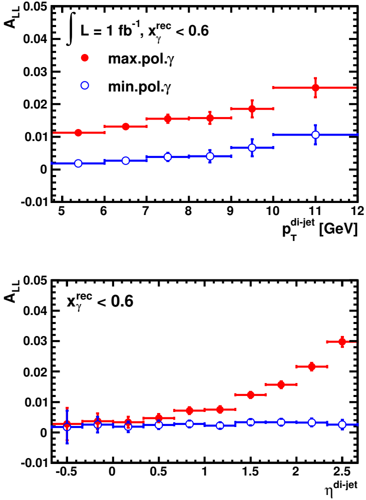

The difference between max.pol. photon and min.pol. photon can be measured in experiment, the pol.photon PDFs can be constrained at EIC.

Underlying events: region method

Underlying events: everything except the particles fragmented from the hard scatted partons.

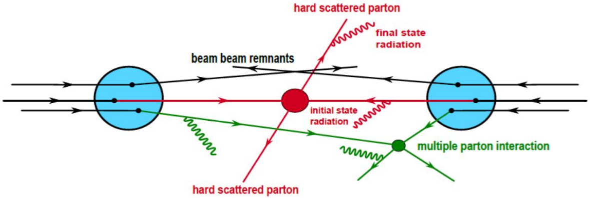

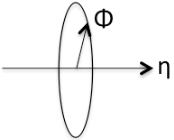

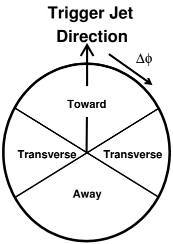

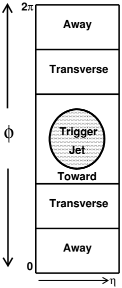

Three regions: $(\Delta\Phi = \Phi_{\text{part}} - \Phi_{\text{Jet1}})$

- Toward: $|\Delta\Phi| < 60^\circ$
- Transverse: $60^\circ < |\Delta\Phi| < 120^\circ$
- Away: $|\Delta\Phi| > 120^\circ$

Measurments:

- Charged multiplicity density, sum pt density Versus $\Delta\Phi$
- Charged multiplicity density, sum pt density Versus p_T^{Jet1}

Results from region method

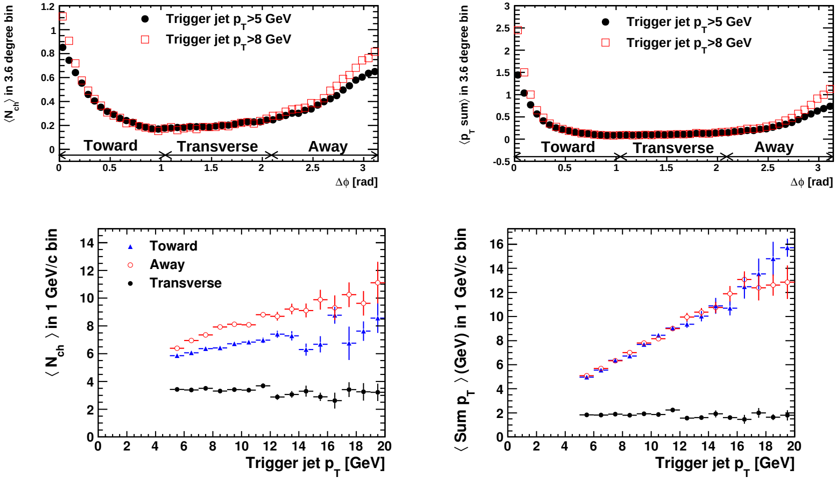

Off-axis method

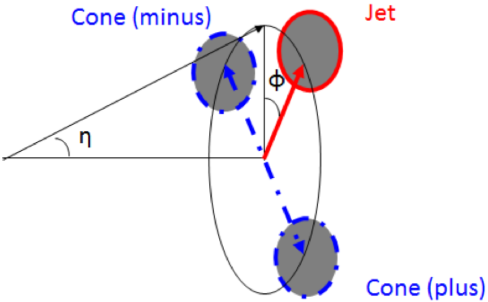

- Look at jets with high momentum, jet by jet
- Two off-axis cones are centered at the same η as the jet but $\pm\pi$ away in Φ from the jet
- Take the particles inside the cones as from underlying events. By using this method, the dependence on η is considered.

Comparison of the two methods

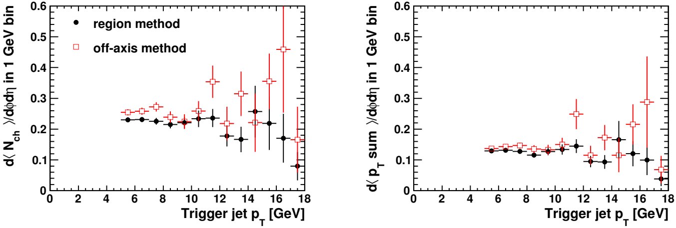

- Results from two different method are consistent, the dependence on η is minor
- The underlying event effect from EIC is comparable with the results from $\sqrt{s} = 250$ GeV pp collisions at STAR

Proton PDFs extracted from inclusive CC ep scattering

High x and high Q^2 events

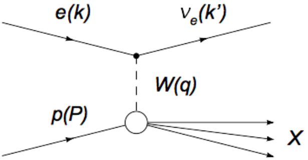

- The reduced cross section for inclusive Charged Current ep scattering are defined as $\sigma_{r,CC} = \frac{2\pi x_{Bj}}{G_F^2}[\frac{M_W^2+Q^2}{M_W^2}]^2 \frac{d^2\sigma_{CC}}{dx_{Bj}dQ^2}$, in HERAFitter, the value of $G_F = 1.16 \times 10^{-5}$ GeV^2 and $M_W = 80.385$ GeV.
- CC structure function are defined as $\sigma^-_{r,CC} \approx (xU + (1-y)^2 x\bar{D})$, $U = xu + xc$, $\bar{D} = x\bar{d} + x\bar{s}$

Inclusive cross section

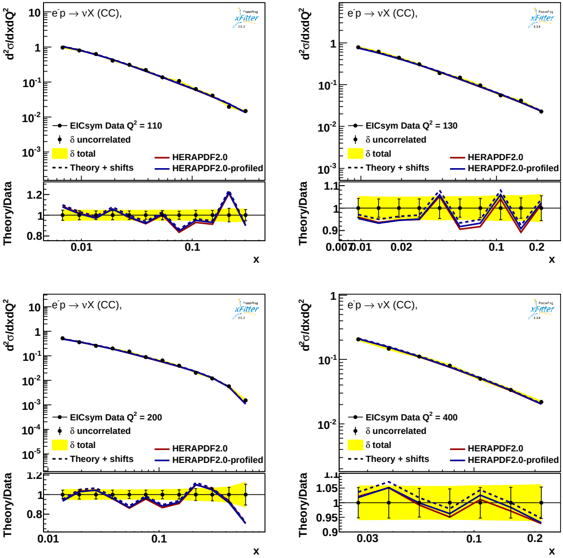

Extracting PDFs by a global fitting

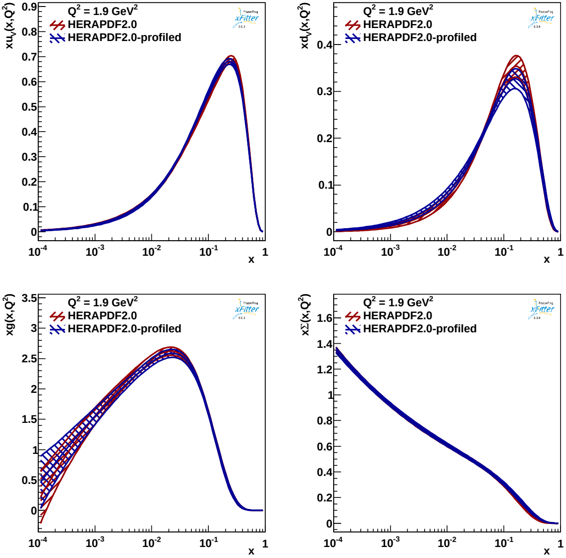

How well can EIC constrain PDFs?

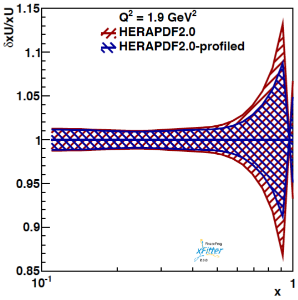

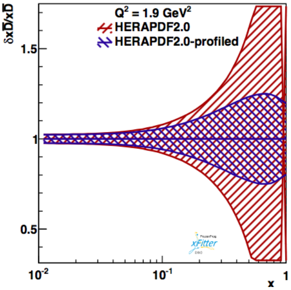

$xU = xu + xc$, $x\bar{D} = x\bar{d} + x\bar{s}$

U and $\bar{D}$ are better constrained compared with HERA

Summary and outlook

The EIC will profoundly impact our understanding of QCD and its dynamics with high luminosity & high energy, nuclei & beam ploarization

- The structure of nucleons and nuclei
- Spin of the proton
- Will enable images of yet unexplored nonlinear regions

Thank you!

back up: The tracking system used in the model detector for eRHIC

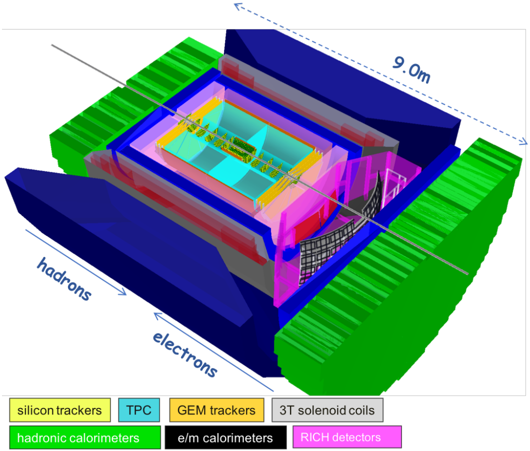

- Time projection chamber (TPC) $|\eta| < 2$
- Silicon trackers $2 < |\eta| < 4$
- Electromagnetic Calorimeter (ECal) $-4 < \eta < 4$
- Hadron Calorimeter (HCal): $1 < |\eta| < 4$

Multivariable-distribution of q/g jet

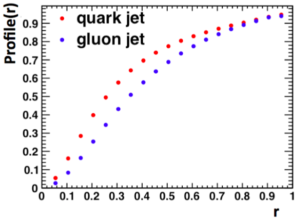

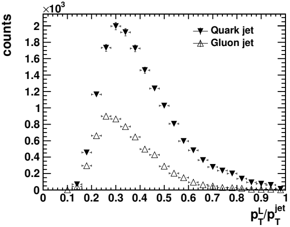

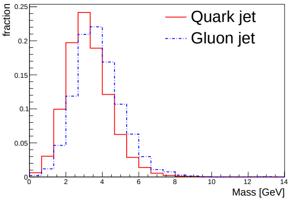

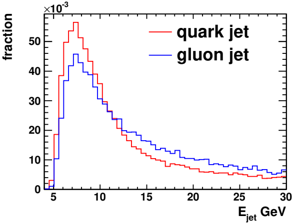

Gluon jets have a more uniform energy fragmentation, while quark jets are more likely to produce narrow jets with hard constituents that carry a significant fraction of the energy.

q/g jet discrimination

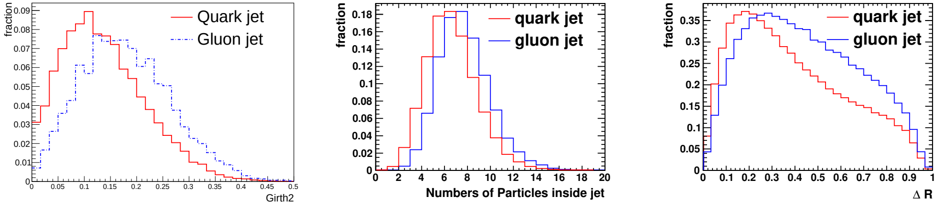

- Some definitions: p_T^L represents the highest p_T of the hadrons inside the jet; Girth2 $= \sum_{i \in \text{cone}} \frac{p_T^i}{p_T^{\text{jet}}} |R_i|^2$; ΔR is the distance between particle and jet axis
- Conclusion: Gluon jets are wider, with higher multiplicities, having a more uniform energy fragmentation, while quark jets are more likely to produce narrow jets with hard constituents that carry a significant fraction of the energy

TMVA method

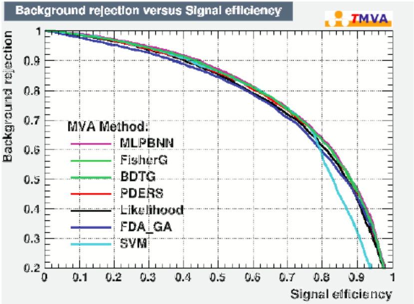

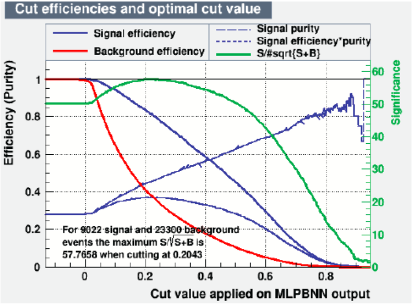

Toolkit for Mulivariate Data Analysis with ROOT (TMVA): for current study, we place cut where signal purity = signal efficiency

Di-jets at EIC from PYTHIA

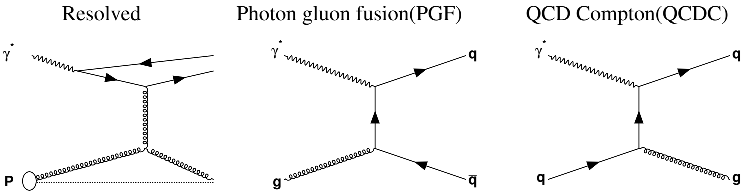

- The resolved, direct (PGF, QCDC) processes can produce di-jets.
- For each di-jet pair, we do geometry match in the simulation, then will know the jet is a quark/gluon jet.

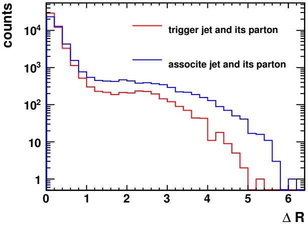

- two output partons → di-jet match in each event, $\Delta R < 1.0$

Jet algorithm

- Clustering Algorithms
  - k_T: $d_i = p^2_{T,i}$,
    $d_{ij} = \min(p^2_{T,i}, p^2_{T,j}) \times \frac{\Delta R^2_{ij}}{R^2} = \min(p^2_{T,i}, p^2_{T,j}) \times \frac{(y_i - y_j)^2 + (\phi_i - \phi_j)^2}{R^2}$, if d_{min}=min(d_i, d_{ij}) is d_{ij}; else, remove j from the list as a jet.
  - anti-k_T: $d_i = \frac{1}{p^2_{T,i}}$, $d_{ij} = \min(\frac{1}{p^2_{T,i}}, \frac{1}{p^2_{T,j}}) \times \frac{\Delta R^2_{ij}}{R^2}$.

  Given $p_{T,j}$ is very small, also $\frac{\Delta R^2_{ij}}{R^2} > 1$:

  anti-k_T: $d_{ij} = \frac{1}{p^2_{T,i}} \times \frac{\Delta R^2_{ij}}{R^2} > \frac{1}{p^2_{T,i}}$.

  It's more likely that j will be a candidate particle for jets by applying k_T algorithm that of anti-k_T. The back reaction sensitivity is highly suppressed by using anti-k_T algorithm in comparison with k_T algorithm.

- Cone-Type Algorithms
  - SISCone: All circles defined by pairs of edge points are all stable cones.

Jet algorithm

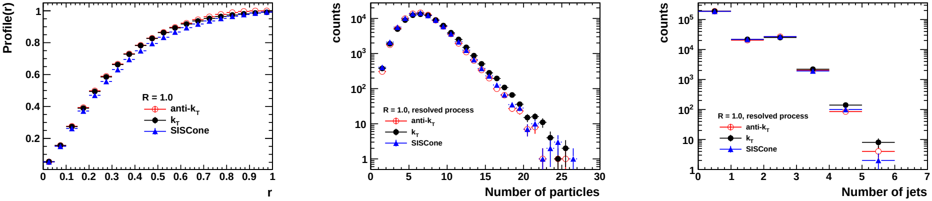

- Some definitions: $Profile(r) = \frac{\sum_{r_i<r} p_T^i}{p_T^{\text{jet}}}$, with drawing a inner cone (r is the radius of this cone,$r = \sqrt{\Delta\eta^2 + \Delta\phi^2}$) inside the jet
- Result: While there are differences in the general behavior of different algorithms, they are relatively minor
- Conclusion: The choice of algorithm will have little impact, anti-k_T algorithm produces the most collimated jets with regular boundaries

Jet definition: jet radius

R=0.4,0.7,1.0. $\hat{s}$ is the input squared invariant mass of the two partons. di-jet mass is reconstructed:

$M = \sqrt{2p_{T1}p_{T2}(\cosh(\Delta\eta) - \cos(\Delta\Phi))}$.

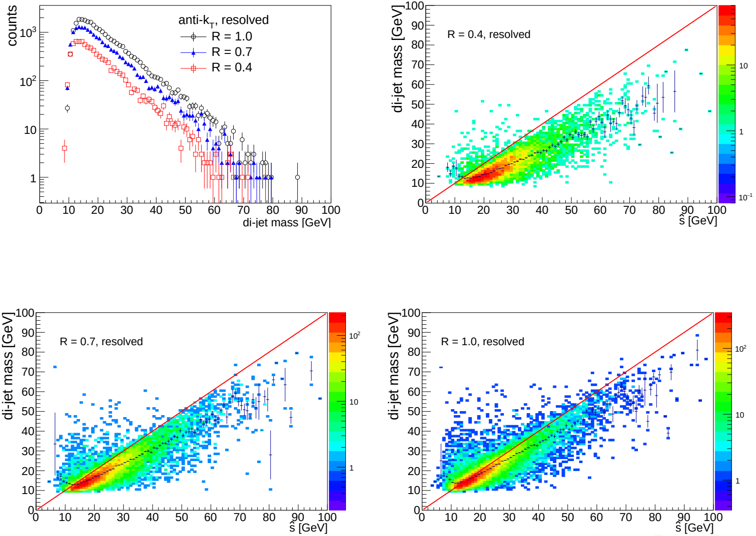

Motivation: Existing photon PDFs

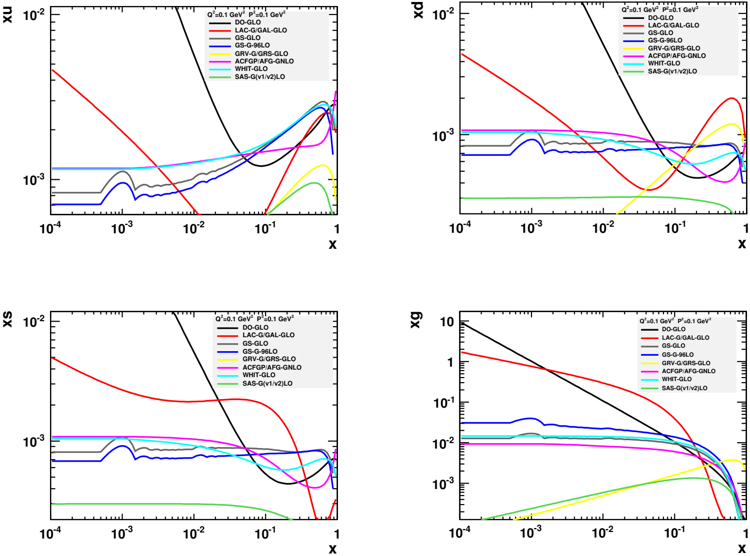

x is the momentum fraction of the parton from the photon, in the following section, it is marked with x_γ